

A Study on enhancing the OFDM Schemes in Wireless Communication

Alagu Harshini.S.¹, Vinothini.K.² and Naveenkumar.R.³

^{1,2} III ECE, Dept. of ECE, VSB College of engineering Technical Campus, Coimbatore

³ Assistant Professor, Dept. of ECE, VSB Engineering College, Karur.

alaguharshiniraji22@gmail.com¹, vinothini96@gmail.com² and naveentamil256@gmail.com³

Abstract

This paper presents enhancing the OFDM schemes in wireless communication techniques for ultra-low power (ULP) devices. The concept of embedded back-channel communication is proposed to enable a variety of new applications by interconnecting heterogeneous ULP devices through existing Orthogonal Frequency Division Multiplexing (OFDM) based WiFi (IEEE 802.11a/g/n/ac) networks. The proposed back-channel communication allows ULP devices to decode messages embedded in WiFi OFDM packets even if these ULP devices are incapable of demodulating OFDM. The proposed back-channel signaling has unique properties that are easily detectable by non-WiFi ULP receivers consuming sub-mW of active power. The proposed scheme eliminates the need for specialized transmitter hardware or dedicated channel resources for embedded back-channel signal transmission. Instead, carefully sequenced data bit streams will generate back-channel messages from already-deployed WiFi infrastructure without any hardware Modification. This paper demonstrates that WiFi OFDM back-channel communication is feasible in various modulation formats such as pulse position modulation (PPM), pulse phase shift keying (PPSK), or frequency shift keying (FSK). Systematic algorithms are unveiled to create back-channel messages in various modulation formats from a WiFi standard compliant datapath. Comprehensive bit error rate (BER) performance analysis of various WiFi back-channel communication schemes is derived and validated in realistic multipath frequency selective fading channels. so the most important aspect of this proposed work is latency and energy consumption so ULP is efficiently implemented in order to provide the optimize and efficient OFDM schemes in wireless communication.

Keywords: ULP, OFDM, BER, WIFI

I. INTRODUCTION

In modern ultra-low power (ULP) wireless Internet-of-Things (IoT) applications, wireless communication is typically the dominant factor in overall power consumption [1] - [3]. Realizing energy-efficient wireless communication, therefore, is the most critical issue to prolong the lifespan of extremely energy- / power-constrained ULP IoT devices.

This paper presents a new concept of back-channel communication embedded in standard compliant wireless packets. We consider the Orthogonal Frequency Division Multiplexing (OFDM) [4] based WiFi (IEEE 802.11 a/g/n/ac) [5] as the primary target wireless standard although the proposed technique can be generalized for other standards as well. The proposed back-channel communication does not require specialized hardware or a dedicated wireless channel to send back-channel signals embedded in standard compliant packets. Instead, carefully crafted bit sequences in the data message would generate embedded back-channel signals. That is, back-channel signal transmission is entirely software-defined by

simply using a proper data bit sequence on standard compliant packets without modifying already-deployed hardware infrastructure.

Demodulating a WiFi OFDM signal is a power demanding task (typically 120mW [7] - [8]) due to stringent RF / analog frontend specifications and sophisticated digital baseband processing. Although WiFi signals are ubiquitously available in urban environments, the majority of ULP IoT devices cannot utilize WiFi connectivity because of their extremely limited power and/or complexity budget [1] - [3], [9], [10]. The proposed back-channel communication technology will break this barrier to allow heterogeneous ULP IoT devices to interoperate with already existing WiFi infrastructure with minimal power consumption. [6] discussed about Improved Particle Swarm Optimization. The fuzzy filter based on particle swarm optimization is used to remove the high density image impulse noise, which occur during the transmission, data acquisition and processing.

Prior works [11] [12] demonstrated a primitive back-channel communication concept in the form of packet length modulation or packet interval modulation using multiple consecutive WiFi or Bluetooth Low Energy (BLE) packets. The packet length or interval modulation utilizes an entire packet (or multiple packets) as an on-off-keying information symbol for the energy detector based receiver. Its efficiency, however, is very poor since the signaling requires many consecutive packets. Moreover, this form of back-channel signaling is particularly vulnerable to interferences as the packet length modulation [11] is susceptible to an interferer OFDM packet (or any other high power interference signal) that could appear between multiple back-channel signaling packets. The WiFi/BLE packet collision (which is common in the collision avoidance based medium access control scheme) can disrupt the packet length or interval modulation too. The other related technique is the hierarchical modulation [13] [14] [15]. In hierarchical modulation, receivers can selectively demodulate high rate (e.g., 16QAM) or low rate (e.g., 4QAM ignoring 2 LSBs out of 16QAM) information from a single packet depending on the channel quality. Unlike our proposed back-channel scheme, however, this hierarchical modulation scheme does not allow communication among heterogeneous devices using very distinct modulation schemes (e.g., coherent vs. non-coherent).

This paper demonstrates intra-packet back-channel modulation schemes and the feasibility of the embedded back-channel signal generation without modifying the existing packet structure

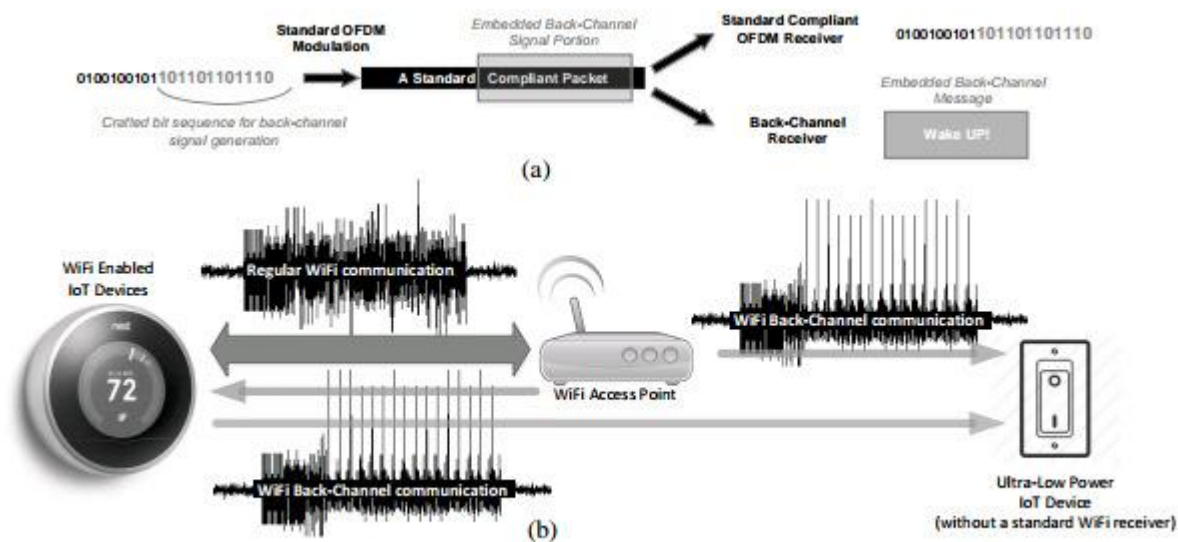


Fig. 1. Concept of WiFi back-channel communication

of WiFi standards. Embedded back-channel signals are all generated by a set of carefully crafted bit sequences within the boundary of standard compliant packet structure. The proposed back-channel communication concept is depicted in Fig. 1 –(a)

A standard compliant data receiver can demodulate the entire bit sequence including the bits to create back-channel message. Meanwhile, at the ULP back-channel receiver, only the embedded back-channel message is decodable, not the entire bit sequence.

The back-channel signaling must be accomplished within strict constraints of the standard compliant packet structure. This paper discusses systematic methods to generate a subset of unique bit sequences that will embed desired back-channel signals in WiFi packets using pulse position modulation (PPM), pulse phase-keying (PPSK), and frequency shift keying (FSK) formats. This back-channel concept can be extended and generalized to other OFDM based communication systems such as the cellular 4G LTE (long-term evolution). Therefore, the proposed back-channel technique could directly impact the next wireless standardization to adopt more flexible packet structures to enrich use-cases of back-channel communication.

The comprehensive low power wireless transceiver survey [16], Fig. 2, indicates that the state-of-the-art ULP transceivers are capable of operating at 95 dBm received signal sensitivity level with sub-mW of active power consumption. It is worth noting that almost all sub-mW transceiver IC designs in Fig. 2 employ either FSK, single carrier PSK, or non-coherent energy detection based schemes such as on-off keying to achieve the lowest power consumption given a target sensitivity level. The state-of-the-art 2.4GHz carrier frequency ULP FSK, PSK, energy-detection receiver designs [17], [18], [19] respectively report 350 W , 2.4mW , and 415 W power consumption for -86dBm, -92dBm, and -87dBm sensitivity with 1Mbps, 2Mbps, and 250kbps data rate. Meanwhile, commercial / academic WiFi OFDM ICs [7] - [8] aim for a very different class of applications where tens of Mbps data rates are necessary, and hundreds of mW power consumption is affordable.

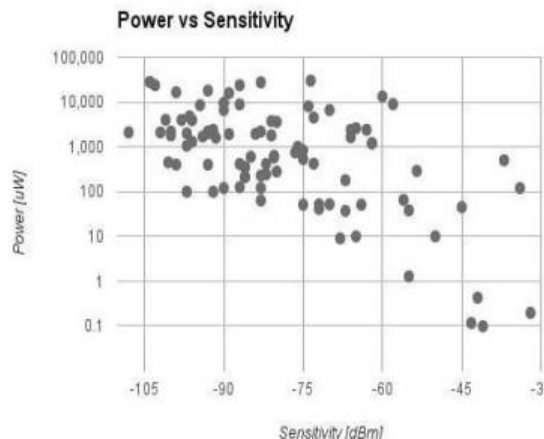


Fig. 2. ULP radio survey. Sensitivity vs Power consumption tradeoff.

The proposed back-channel communication provides an unique engineering solution to bridge the power and data rate mismatch between the WiFi and ULP IoT devices. We will discuss in Section IV potential architectures to realize ULP back-channel receivers that could operate with less than a few mW of power budget to demodulate PPM, PPSK, or FSK messages embedded in WiFi OFDM packets.

We will discuss in-depth theoretical analysis on bit error rate (BER) performance for various back-channel communication modulation schemes. Realistic multi-path frequency selective fading channels are applied to derive back-channel BER expressions in Section V. The BER performance analysis reveals that back-channel modulation schemes can provide significant signal-to-noise ratio (SNR) gain over conventional WiFi OFDM by lowering the effective symbol rate and concentrating the OFDM symbol power on intentionally generated sparse pulses (PPM and PPSK).

ULP back-channel receivers can exploit this SNR gain to achieve significantly longer link distance and/or lower power consumption than what conventional WiFi OFDM communication can offer.

We envision that the proposed back-channel technique can be best utilized as a wireless paging / wakeup / interrupt channel empowered by already deployed legacy WiFi devices as depicted in Fig. 1 - (b). The back-channel signaling allows an existing WiFi device to control heterogeneous ULP devices

that employ various types (e.g., PPM, PPSK, FSK, etc.) of back-channel receivers with a dramatically lower power budget than what a conventional WiFi receiver requires. The proposed back-channel technique also provides a unique solution to realize the concept of 'WiFi on-demand', in which the power-demanding OFDM receiver stays in deep-sleep, rather than continuously searching for randomly arriving packets, until it is asynchronously (and remotely) activated by the paging / wakeup message delivered to an always-on ULP back-channel receiver.

This paper is organized as follows. In section II, we discuss general procedures to create back-channel modulations embedded in OFDM packets. Section III presents systematic algorithms to generate back-channel messages complying with the WiFi standard datapath. Potential ULP architectures for WiFi back-channel receivers are proposed in Section IV. Section V provides in-depth BER analysis of various WiFi back-channel modulation schemes. In section VI, we evaluate WiFi back-channel modulation schemes with BER simulations and analysis results. Section VII concludes the paper.

II. BACK-CHANNEL MODULATIONS REALIZED IN OFDM

In OFDM, the information bits are modulated using a linear modulation scheme such as quadrature amplitude modulation (QAM) on each subcarrier with equal average power, resulting in a white (or flat) frequency spectrum power spectral density

(PSD) over the channel bandwidth. This white PSD property makes the OFDM time domain signal appear as an uncorrelated noise-like signal with relatively high peak-to-average power ratio (PAPR). This high PAPR, in fact, is one of the major drawbacks of OFDM [20] since it requires highly linear RF circuits over a wide dynamic range to avoid unintended signal quality degradation from non-linear distortion. In this section, we discuss pulse based back-channel modulation techniques that utilize the high-PAPR OFDM property as a controlled modulation scheme for communication. In addition, a frequency domain back-channel modulation scheme that intentionally creates non-uniform PSD to emulate FSK is discussed in this section.

A. Pulse Position Modulation (PPM) Back-Channel

The pulse position modulation (PPM) back-channel uses the position of pulses (1 pulse per OFDM symbol) to convey

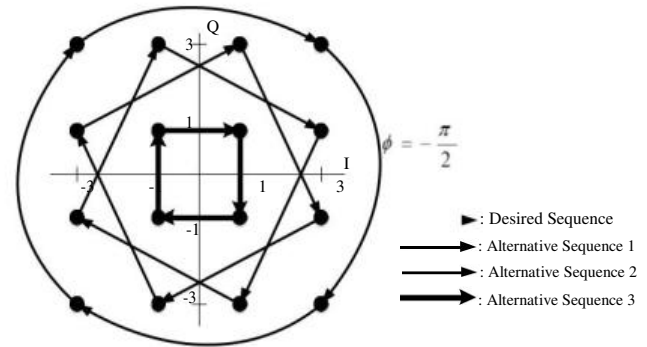
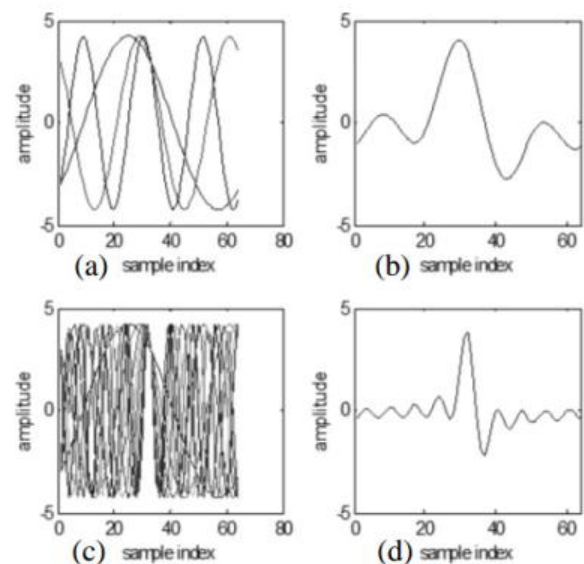


Fig. 3. Back-Channel pulse generating symbol sequence examples using 16-QAM

back-channel messages. Since the SNR of the PPM back-channel is enhanced by maximizing the power of the intentionally created back-channel pulse, the PPM back-channel communication purposely maximizes the PAPR of the OFDM time domain signal. Fourier transform theory [21] indicates that the PAPR of an OFDM symbol is maximized by assigning linear modulation symbols on subcarriers with a constant phase rotation rate across all subcarriers as in (1).

By selecting a specific in (1), one can adjust the position of a pulse within a time-domain OFDM symbol. A binary PPM embedded in OFDM is realized by using two pulse positions; pulse 0 or pulse 1 resulting from phase rotation rates of p_0 and p_1 respectively, and by selecting one of two pulses depending on the message to be conveyed in back-channel modulation. It is possible to generate a longer pulse with lower peak power using a dithering phase rotation rate. Notice non-zero power, noise-like samples at non-pulse positions in Fig. 4, although the procedure given



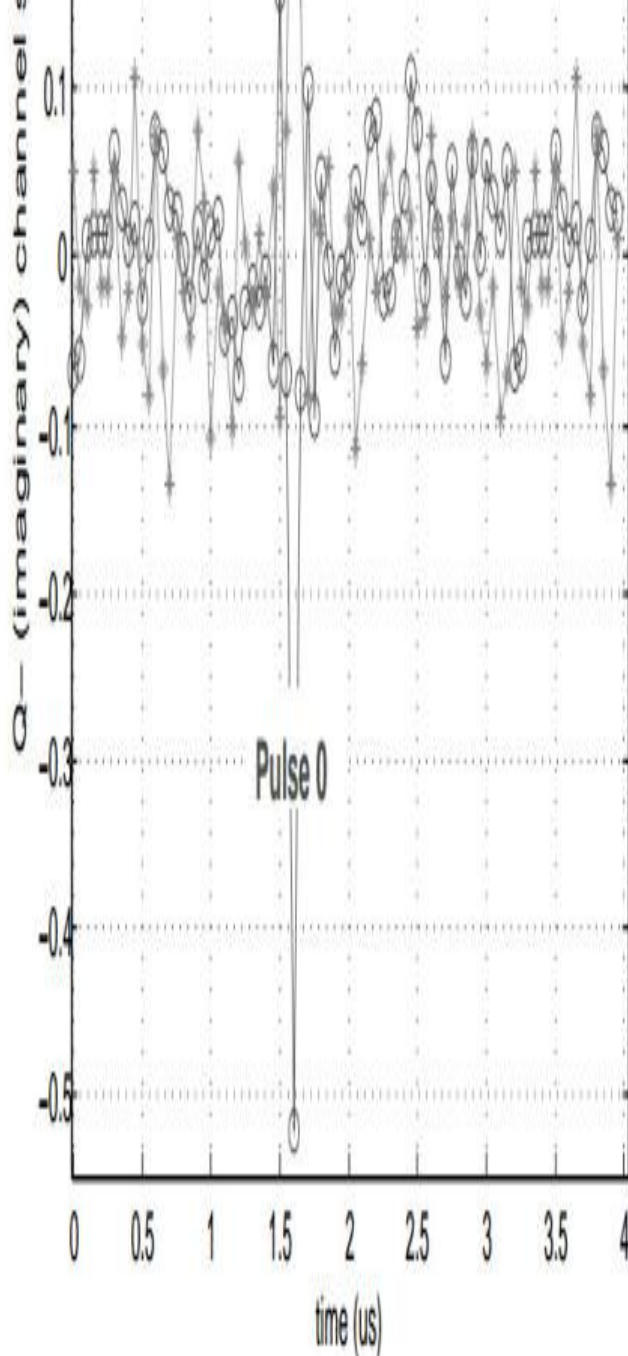


Fig. 5. Realization of binary PPSK back-channel modulation

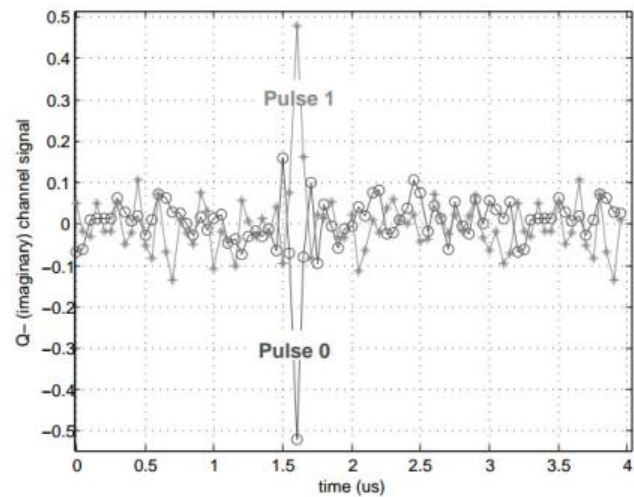
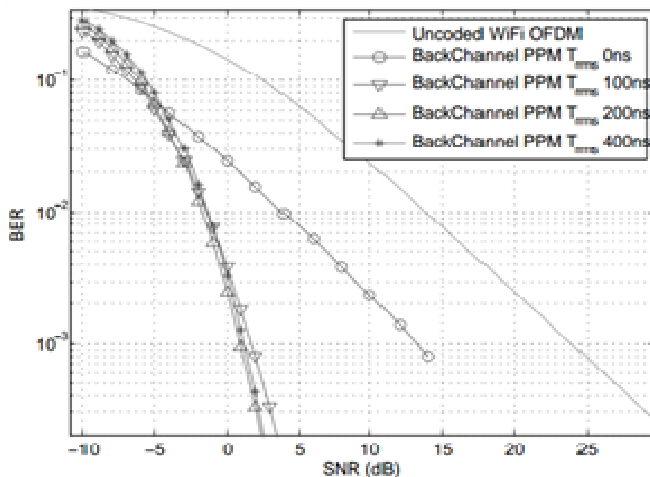


Fig. 5. Realization of binary PPSK back-channel modulation.

III. BACK-CHANNEL MODULATIONS IN STANDARD-COMPLIANT WiFi PACKETS

Thus far, it was assumed that an arbitrary sequence of linear modulation symbols satisfying (1) and/or intentional non-uniform power could be allocated to OFDM subcarriers to generate the desired back-channel modulated signals embedded in OFDM packets.

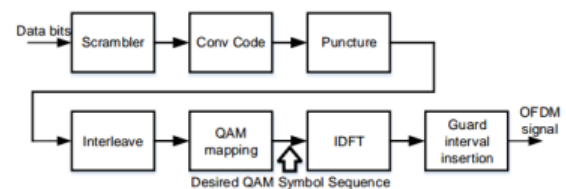


Fig. 7. IEEE 802.11 a/g/n WiFi modulation datapath

The IEEE 802.11 a/g/n WiFi standard datapath shown in Fig. 7, however, does not allow an arbitrary sequence of linear modulation symbols. The input data bit stream is scrambled, and encoded with a convolutional code. The coded bit sequence is then punctured, interleaved, and finally mapped to linear modulation symbols in the WiFi standard datapath. The linear modulation on each subcarrier is either BPSK, QPSK (4-QAM), 16-QAM, or 64-QAM. Some subcarriers are assigned as pilot and null subcarriers with predefined modulation symbols. Therefore, only a subset of all possible QAM symbol sequences is WiFi standard compliant. The proposed method circumvents this issue using the fact that the scrambler, interleaver and QAM mapper in WiFi standards are all one-to-one mapping invertible functions. The puncturing operation can be disabled in some WiFi modes without affecting the bit sequence. Even if the puncturing is enabled, the back-channel modulation process can simply allocate arbitrary bits on punctured bits as they will be eventually removed before the QAM mapping. In fact, it is only the



convolutional encoder and the deterministic null/pilot subcarrier mapping that prevent creating an arbitrary sequence of QAM symbols. The convolutional encoder output has to be a valid codeword, which is a subset of all possible bit sequences.

A. Pulse Based Back-Channel Modulation Using WiFi Data-path

The property of a back-channel modulated pulse within an OFDM symbol is determined by the constant phase rotation rate and the initial symbol X_1 in (1). Once an OFDM symbol is assigned with a specific X_1 for pulse-based back-channel modulation, the desired QAM symbol sequence for all subcarriers within an OFDM symbol; $Q_1; Q_2; \dots; Q_K$ are obtained by (1). In general, this desired QAM symbol sequence is infeasible to be realized in a WiFi compliant datapath. We propose a systematic procedure specified in Algorithm 1 that utilizes multiple (R) alternative QAM symbol sequences with the same but with different starting symbols $X_1^{(r)}$ as depicted in Fig. 3. R alternative sequences are generated with the rule of $jX_1^{(1)} X_1 j jX_1^{(2)} X_1 j \dots jX_1^{(R)} X_1 j$. Algorithm 1 allows deviation from the desired QAM symbol sequence and temporary switching to one of alternative sequences if that is necessary to enforce the resulting sequence is standard compliant. The alternative sequences are sorted in the order of minimizing the impact of deviation from the desired sequence. Algorithm 1 specifies the detailed procedure to produce pulse-based (PPM or PPSK) back-channel modulation complying with WiFi standards.

Algorithm 1 WiFi Data Bit Assignment for Pulse Based Back-Channel Modulation

1. A WiFi packet must start with mandatory header bits and service bits. The first OFDM data symbol is encoded using header bits. The second OFDM data symbol consists of service bits and arbitrary padding bits. The exact state of the scrambler and convolutional encoder after the second OFDM data symbol modulation is recorded for back-channel modulation starting from the third OFDM data symbol.
2. For a back-channel modulated OFDM symbol, the desired sequence of QAM symbols is generated using (1).
3. Generate multiple (R) alternative QAM symbol sequences with the same but with a different starting symbols $X_1^{(r)}$ satisfying $jX_1^{(1)} X_1 j jX_1^{(2)} X_1 j \dots jX_1^{(R)} X_1 j$.
4. For both desired and alternative sequences, QAM symbols that belong to pilot or null subcarriers are replaced by WiFi standard defined pilot and null symbols.
5. Desired and alternative sequences are converted to corresponding bit sequences at the convolutional encoder output (Fig. 7) using inverse operations of QAM mapping, interleaving, and puncturing. These bit sequences are denoted by the desired coded-bit sequence and alternative coded-bit sequences.
6. N_{SI} bits at the scrambler input are required to create an OFDM symbol. These data bits, $b_j; j = 0; 1; \dots; N_{SI} - 1$, are sequentially determined from the lowest index $j = 0$. Each b_j has two possible values; 0 or 1.

while $j < N_{SI}$ do if $b_j = b; b \neq 0$; lg maps to the desired coded bit sequence after scrambling and convolutional encoding
then

7-a. $b_j < b^*$. else {neither $b_j = 0$ nor 1 maps to the desired coded bit sequence}

7-b. b_j is assigned with the value that provides an alternative coded bit sequence with smallest index r . If all alternative coded bit sequences are infeasible, b_j is assigned with a random value.

end if

8. Update the state of the scrambler and convolutional encoder according to b_j .

9. $j = j + 1$

end while

10. Repeat from the step 2 if there are more back-channel symbols to be modulated. If not, quit.

B. FSK Based Back-Channel Modulation using WiFi Datapath

The ideal M-ary FSK back-channel modulation on OFDM requires controlling symbol power on M non-overlapping subsets of subcarrier indices $S_{SC}^{(0)}; S_{SC}^{(1)}; \dots; S_{SC}^{(M-1)}$ as described in Section II. Although ideal M-ary FSK modulation is infeasible due to WiFi datapath restrictions, a systematic method described in Algorithm 2 circumvents this issue to generate approximated FSK back-channel modulation that is compliant with WiFi standards.

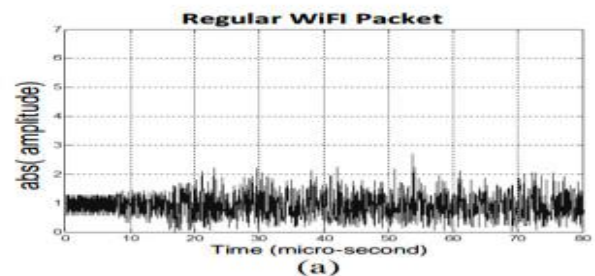
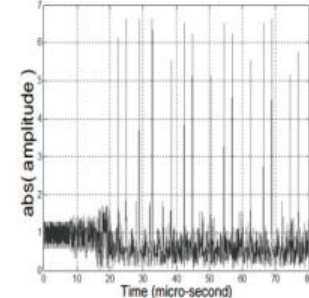
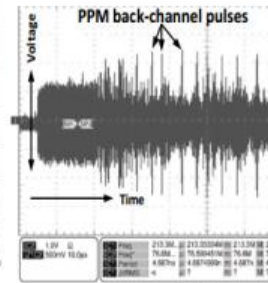


Fig. 8. Pulse-based back-channel modulation on WiFi packets using Algorithm1. (a) a conventional WiFi packet; (b) a MATLAB simulated WiFi packet with PPM back-channel modulation; (c) a WiFi packet from a commercial transceiver chipset with embedded PPM back-channel

WiFi Packet with Embedded Back-Channel in PPM



(b)



(c)

WiFi packets using Algorithm1. (a) a conventional WiFi packet; (b) a MATLAB simulator from a commercial transceiver chipset with embedded PPM back-channel modulation.

IV. LOW POWER, WiFi BACK-CHANNEL RECEIVER ARCHITECTURES

One of main motivations of the back-channel modulation is to realize ULP receivers with dramatically reduced power consumption compared to a conventional OFDM receiver. Power demanding quadrature demodulation, a high accuracy RF local oscillator (LO) phase-lock loop (PLL), and DFT/FFT baseband processing are all unnecessary for PPM based backchannel demodulation. In this section, we propose receiver architectures that are suitable for extremely power-limited, non-WiFi compliant ULP devices to demodulate back-channel signals embedded in OFDM packets. Fig. 9 depicts potential ULP receiver architectures for various types of back-channel modulations.

The architectures shown in Fig. 9 (a) and (b) are designed for PPM back-channel signals. They are based on non-coherent signal envelope detection which does not require costly RF frequency synthesizers or mixers. The envelope of the signal is converted to digitally quantized levels to be processed in the digital baseband. Envelope detection is typically implemented with a rectifier or by self-mixing (squaring operation) followed by a low pass filter. The RF bandpass filter (BPF) and the amplifier are employed at the beginning of the datapath for interference rejection and out-of-band noise filtering.

For further power consumption reduction, signal envelope detection and analog-to-digital converter (ADC) in Fig. 9 (a) can be replaced by a rectifier followed by a binary signal level comparator as shown in Fig. 9 (b) where pulse detection is performed entirely in analog circuits using a predefined pulse voltage bias (V_{bias}).

Since the amplitude information is lost during analog one-bit comparator quantization, its bit error rate performance is expected to be significantly worse than that of the architecture employing an ADC (Fig. 9 (a)). Nonetheless, for applications that operate only in short distances, the architecture given in Fig. 9 (b) could be a compelling, energy-efficient solution. A ULP receiver design [22] that employs a similar rectifier based architecture reports 116nW power consumption. Meanwhile, the PPSK back-channel receiver architecture proposed in Fig. 9 (c) utilizes the same RF / analog front-end for coherent quadrature demodulation that is required for conventional single-carrier PSK or OFDM demodulation. Unlike OFDM demodulation, the baseband signal processing for PPSK back-channel does not involve costly DFT/FFT computation and its symbol rate is at

least 1=64 times lower than the OFDM signal bandwidth. Thus, its complexity (and power consumption) is significantly lower than that of a conventional WiFi OFDM receiver.

Although its complexity is higher than that of non-coherent architectures designed for PPM back-channel, analysis in Section V and VI reveals that the PPSK back-channel has superior bit-error rate performance compared to PPM based back-channel modulation. Fig. 9 (d) depicts the proposed ULP receiver architecture to demodulate the FSK modulated back-channel. This noncoherent receiver architecture consists of bandpass filters, power detectors, integrators (lowpass filters), and a comparator to detect power difference between two outputs from nonoverlapping bandpass filters. The digital baseband processing produces the final demodulated bits by sampling the comparison output at the Nyquist rate.

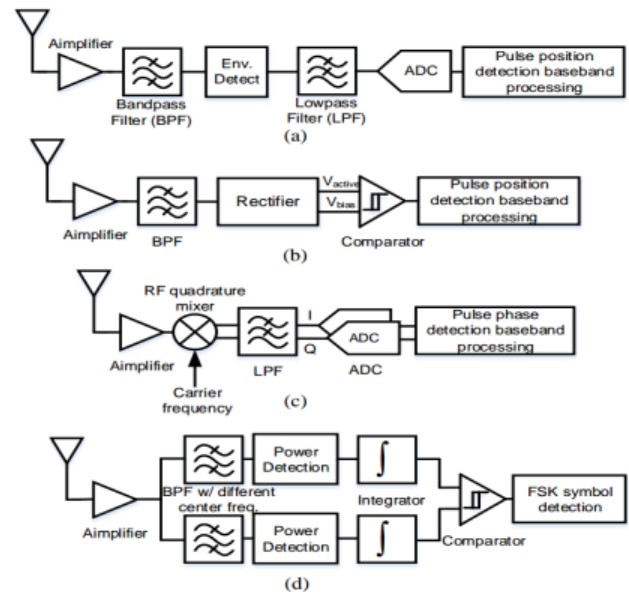


Fig. 9. OFDM back-channel receiver architectures. (a) Non-coherent PPM back-channel receiver; (b) Simplified, non-coherent PPM back-channel receiver; (c) coherent PPSK back-channel receiver; (d) Non-coherent FSK back-channel receiver.

V. BACK-CHANNEL COMMUNICATION ERROR RATE PERFORMANCE ANALYSIS

In this section, we analyze the error rate performance of the back-channel receivers discussed in Section IV. We assume non-coherent energy detector based architectures; Fig. 9 (a) and (d) with ideal circuits and filters for PPM and FSK back-channel BER evaluation respectively. The architecture Fig. 9

(c) with ideal components is assumed for PPSK back-channel performance analysis.

We use a multi-path (frequency selective) quasi-static Rayleigh fading channel model with exponentially decaying power profile, whereby the channel is static within the duration of a single packet but is independent from one packet to the next [23]. Discrete signal model with Nyquist sampling period $T_s = 50\text{ns}$ for 20MHz bandwidth operation is used throughout this section.

The channel impulse response has the form of (2), where h_1 is an i.i.d. zero-mean complex Gaussian random variable with variance

$h_l(3)$, l is the sample index, L is the channel length, and

RMS is the root-mean-squared (RMS) delay spread of the multi-path channel.

We first derive the conventional uncoded OFDM bit error rate (BER) for BPSK modulation on each subcarrier to make a comparison with various back-channel modulation schemes. The DFT operation on the multi-path Rayleigh fading channel (2) results in statistically identical but correlated Rayleigh fading channel for each subcarrier. The average unit power of the channel (3) indicates that the frequency domain channel coefficient for each subcarrier is a complex Gaussian random variable with unit variance. Uncoded system BER is dictated by the distribution of each individual subcarrier channel, and it is independent of correlation among subcarriers because bit errors on a certain subcarrier do not affect bit decisions on the other subcarriers. Although subcarrier channels are correlated, each individual subcarrier experiences the statistically identical Rayleigh flat fading channel [24]. Therefore, the BER of BPSK modulated OFDM subcarriers in our multi-path Rayleigh fading channel model can be obtained.

VI. EVALUATION RESULTS

A. Evaluation Packet Structure

The proposed back-channel scheme enables the packet-in-packet structure as depicted in Fig. 11. This packet structure allows sending messages to both a regular WiFi receiver and a back-channel receiver using a single WiFi packet. The message targeting a regular WiFi receiver is encoded in WiFi symbols in Fig. 11. One WiFi OFDM symbol contains numerous (at least 48) information bits, and its uncoded BER performance is governed by (4) for BPSK. These information bits contained in regular WiFi symbols are ignored by back-channel receivers. Meanwhile, each back-channel symbol in Fig. 11 contains only one information bit (assuming binary PPM, PPSK, or FSK back-channel) per OFDM symbol. These back-channel symbols are intended for back-channel receivers. The uncoded BER of these back-channel symbols can be obtained by (10), (12), and (15). It is worth noting that a regular WiFi receiver can demodulate OFDM symbol input bits (not back-channel information bits) contained in back-channel symbols as they are also valid OFDM symbols. Its BER would be the same as the conventional WiFi OFDM system. However, the decoded bits will be meaningless to regular WiFi receivers because the sole purpose of these bits is to modulate back-channel symbols, not to convey meaningful information for regular WiFi receivers. In order to ensure interoperability, it is desired to assign extra information bits in the WiFi symbol to indicate the presence of back-channel symbols in the packet so that a regular receiver can ignore back-channel modulated symbols for decoding. The packet-in-packet structure in Fig. 11 ends with a regular WiFi symbol which contains the cyclic redundancy check (CRC) bits for the entire packet. In this way, the entire packet is regarded as a valid WiFi packet by regular WiFi receivers without a CRC error.

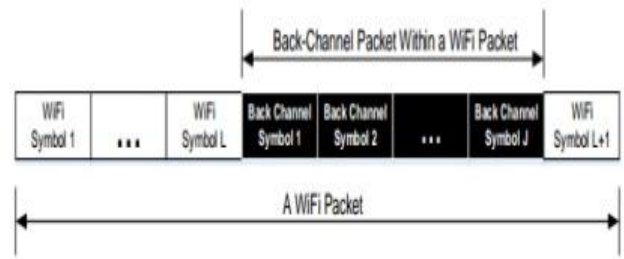
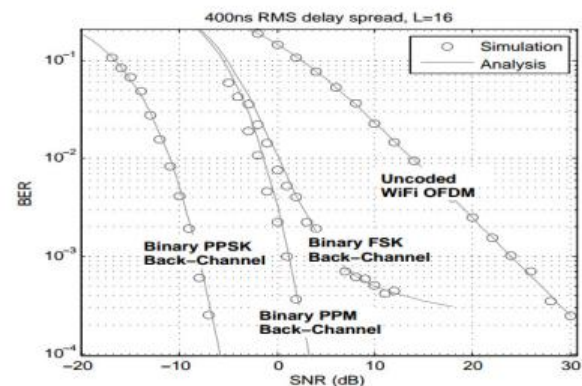


Fig. 11. Evaluated packet structure. A back-channel packet is embedded in a WiFi packet.

B. Performance Evaluation

To validate the back-channel BER analysis, we compared Monte-Carlo MATLAB simulations with the analytical expressions given by (4), (10), (12), and (15). Fig. 12 shows a side by side comparison of the BER performance, and it confirms that analysis results are well matched to the actual BER for various back-channel modulation schemes.

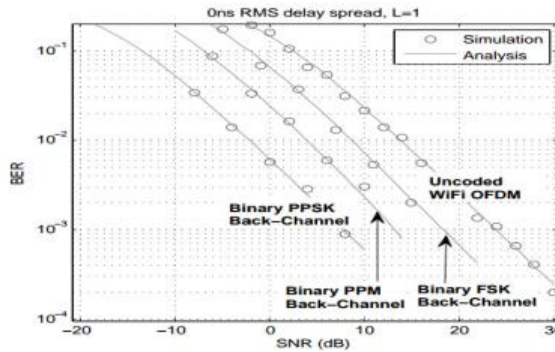
The WiFi standards are designed to operate with up to 800ns (OFDM symbol guard interval length) of channel delay spread. We evaluated $RMS=0$ (Rayleigh flat fading channel), 100, 200 and 400ns RMS delay spread channels with $L=1, 5, 8, 12$, and 16 respectively.



12 (a)

Fig. 12. Uncoded OFDM and back-channel BER performance, MATLAB simulations vs. analysis results. (a) in 400ns RMS delay spread channel; (b) in 0ns RMS delay spread channel.

Fig. 12 shows $RMS=0$ and 400ns results revealing that proposed back-channel modulation schemes can operate with lower SNR than what conventional WiFi OFDM requires. It is because the effective back-channel symbol rate is much lower than the OFDM bandwidth, and back-channel schemes aggregate OFDM symbol energy from 64 subcarriers to create a single back-channel symbol at lower symbol rate. This can be considered as de-spreading gain that is available in spreading spectrum modulation schemes.



12(b)

The back-channel signal bandwidth is 20MHz but the symbol rate is only 250kHz. The SNR gain from this energy concentration or de-spreading is approximately (not exactly because of WiFi compliant datapath requirements) $10\log_{10}64 = 18\text{dB}$ which can be observed by comparing the BER performance between PPSK back-channel and conventional WiFi OFDM (uncoded) in the Rayleigh flat fading channel (Fig. 12 (b)). The BER performance gap is smaller for PPM and FSK back-channel schemes because they use sub-optimal non-coherent demodulation architectures. The BER performance gap increases for a non-zero delay spread channel (Fig. 12 (a)) because back-channel modulation schemes can exploit diversity gain from the multi-path channel with independent taps (2) while the uncoded OFDM does not. This significant SNR gain of back-channel schemes can be utilized to lower power consumption of the ULP back-channel receiver or to extend link distance beyond the conventional WiFi range.

Fig. 13 and Fig. 14 show the impact of channel delay spread on PPM and PPSK back-channel schemes respectively. Note that the conventional uncoded OFDM BER performance is independent of channel delay spread since all subcarriers experience statistically identical Rayleigh fading channels although they are correlated in frequency domain.

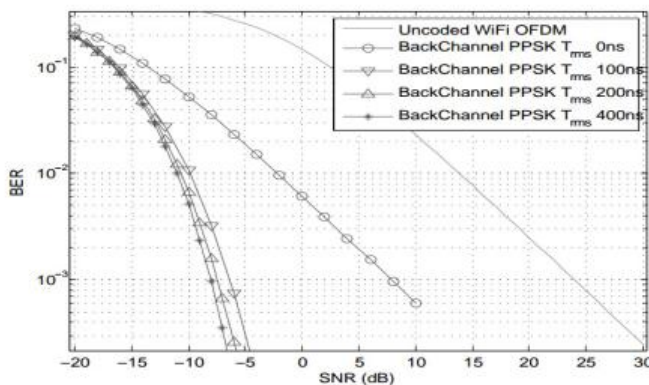


Fig. 14. PPSK back-Channel BER performance in 0, 100, 200, and 400ns delay spread channels.

Fi Fig. 15. FSK back-Channel BER performance in 0, 100, 200, and 400ns delay spread channels

It shows the BER performance of FSK back-channel modulation. Notice channel RMS delay spread dependent error floors (i.e. not improving

On the other hand, PPM and PPSK back-channel schemes gain from multi-path diversity because each channel tap of (2) in the time domain has independent distribution. That is, a low power fading channel tap can be compensated by other high power channel taps with high probability when there are multiple independent fading channel taps in the channel impulse response. It is worth noting that the gain from longer channel response (larger L) is not necessarily monotonic. For instance, the 200ns delay spread channel has slightly better performance than the 400ns channel for PPM as shown in Fig. 13.

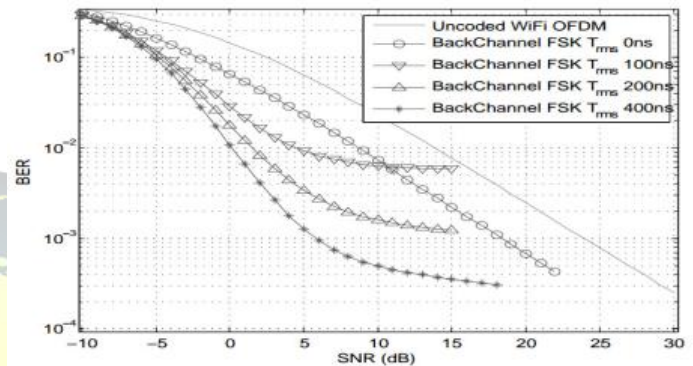
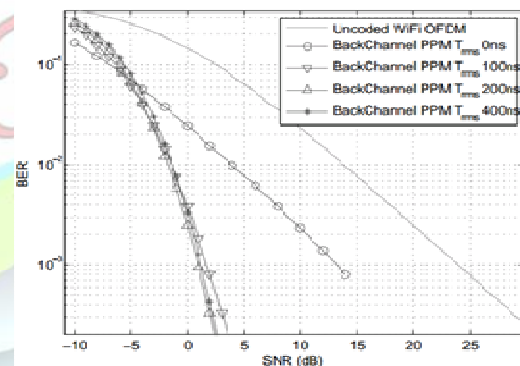


Fig. 13. PPM back-Channel BER performance in 0, 100, 200, and 400ns delay spread channels

The diversity gain diminishes for a large L because the average signal energy remains constant regardless of channel delay spread length in our channel model (2) - (3) while the noise energy observed for symbol detection linearly increases as a function of L .



BER for higher SNR) on the FSK back-channel BER plots. These error floors are because of frequency selectivity of the channel. When high power subcarriers encounter destructive fading, the FSK back-channel error probability increase. The shorter channel delay spread results in a wider channel coherence bandwidth, and consequently, the probability of many high power subcarriers suffering from destructive channel fading at the same time (whereas low power subcarriers see constructive channel fading) increases.

C. Proof of Concept Prototype

A micro-controller (MCU) based PPM back-channel receiver prototype was built and validated. For a proof-of-concept prototype, the RF frontend was assembled with discrete components from Mini-Circuits and a low power TI MSP430 MCU evaluation board [27] that is programmed to receive and decode PPM WiFi back-

channel messages in real time. Fig. 16 shows the prototype receiver system architecture. An off-the-shelf power detector [28] outputs the instantaneous power of the 2.4 GHz WiFi signal and the comparator produces a digital pulse for the MCU whenever the power of the Wi-Fi signal exceeds a predefined threshold.

The MSP430 MCU clock frequency of the prototype system is set to 25MHz clock, which is far insufficient to perform regular 20MHz WiFi OFDM demodulation.

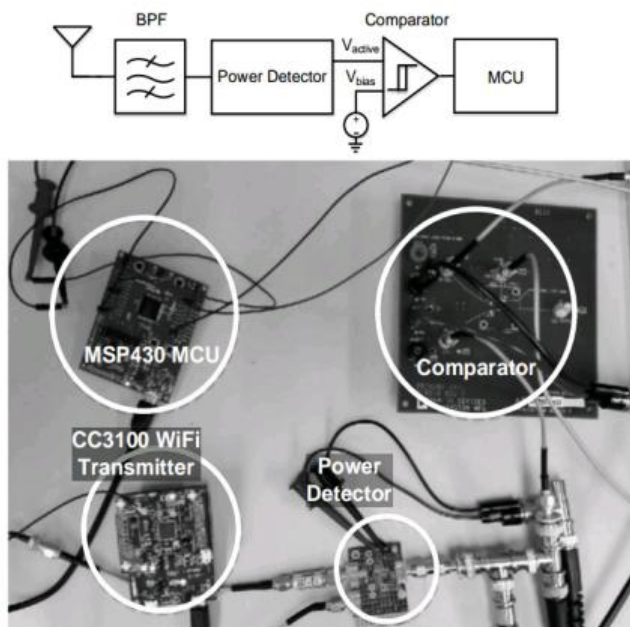


Fig. 16. Proof-of-Concept Prototype System for PPM WiFi Backchannel Reception.

VII. CONCLUSIONS

We presented innovative back-channel communication techniques for ultra-low power wireless devices, which could not afford standard WiFi wireless communication due to their extremely limited power budget. The concept of back-channel communication enables interconnecting heterogeneous ULP devices through existing ubiquitous WiFi networks even if these ULP devices are incapable of decoding regular WiFi messages. The back-channel signaling embedded in WiFi messages has unique properties that are easily detectable by ULP receivers operating with sub mW power budget.

The proposed back-channel scheme eliminates the need for specialized transmitter hardware or dedicated channel resources for embedded back-channel signal transmission. Instead, we have demonstrated that carefully sequenced data bit streams can generate back-channel messages from already-deployed WiFi infrastructure without any hardware modification. Various back-channel modulation formats such as PPM, PPSK or FSK were discussed in this paper.

Theoretical BER analysis revealed that back-channel modulation schemes provide significant SNR gains over the conventional uncoded WiFi OFDM modulation. The impact of

various channel delay spread parameters were analyzed for each back-channel modulation type. Significant SNR gain of back-channel schemes over conventional OFDM can be utilized to lower power consumption of the ULP back-channel receiver or to extend link distance beyond the conventional WiFi range.

The proposed back-channel technique could make direct impact on the next wireless standardization to adopt more flexible packet structures to enrich use-cases of back-channel communication. WiFi standard compliant nodes could potentially benefit from the back-channel technique to significantly enhance their power efficiency without employing a proprietary wakeup signal transmitter and/or dedicated channel resources. Novel concepts such as WiFi-on-demand, replacing conventional always-on WiFi Access Points, can be realized by the outcomes of the proposed technique.

REFERENCES

- [1] I. Demirkol, C. Ersoy, E. Onur, "Wake-up receivers for wireless sensor networks: benefits and challenges," *Wireless Communications, IEEE*, vol.16, no.4, pp.88,96, Aug. 2009.
- [2] L. Gu, J.A. Stankovic, "Radio-triggered wake-up capability for sensor networks," *Real-Time and Embedded Technology and Applications Symposium*, 2004. Proceedings. RTAS 2004. 10th IEEE, vol., no., pp.27,36, 25-28 May 2004.
- [3] J. Ansari, D. Pankin, P. Mahonen, "Radio-Triggered Wake-ups with Addressing Capabilities for extremely low power sensor network applications," *Personal, Indoor and Mobile Radio Communications*, 2008. PIMRC 2008. IEEE 19th International Symposium on, vol., no., pp.1,5, 15-18 Sept. 2008.
- [4] W. Yiyan, W.Y. Zou, "Orthogonal frequency division multiplexing: a multi-carrier modulation scheme," *IEEE Transactions on Consumer Electronics*, vol.41, no.3, pp.392-399, Aug 1995
- [5] IEEE standards association, 802.11n specification, Available at: <https://standards.ieee.org/findstds/standard/802.11n-2009.html>
- [6] Christo Ananth, Vivek.T, Selvakumar.S., Sakthi Kannan.S., Sankara Narayanan.D, "Impulse Noise Removal using Improved Particle Swarm Optimization", *International Journal of Advanced Research in Electronics and Communication Engineering (IJARECE)*, Volume 3, Issue 4, April 2014, pp 366-370
- [7] T.-M. Chen, Y.-M. Chiu, C.-C. Wang, K.-U. Chan, Y.-H. Lin, M.-C. Huang, C.-H. Lu, W.-S. Wang, C.-S. Hu, C.-C., Lee, J.-Z. Huang, B.-I Chang, S.-C. Yen, Y.-Y. Lin, "A Low-Power Fullband 802.11a/b/g WLAN Transceiver With On-Chip PA," *IEEE Journal of Solid-State Circuits*, vol.42, no.5, pp.983 - 991, May 2007
- [8] M. Zargari, S. Jen, B. Kaczynski, M. Lee, M. Mack, S. Mehta, S. Mendis, K. Onodera, H. Samavati, W. Si, K. Singh, A. Tabatabaei, M. Terrovitis, D. Weber, D. Su, B. Wooley, "A single-chip dual-band tri-mode CMOS transceiver for IEEE 802.11a/b/g WLAN," *IEEE International Solid-State Circuits Conference*, 2004. Digest of Technical Papers. ISSCC, Vol.1, 15- 19. Feb. 2004
- [9] G. Chen, H. Ghaed, R. Haque, M. Wiecekowsky, Y. Kim, G. Kim, D. Fick, D. Kim, M. Seok, K. Wise, D. Blaauw, D. Sylvester, "cubicmillimeter energy-autonomous wireless intraocular pressure monitor," *IEEE International Solid-State Circuits Conference*, 2011. Digest of Technical Papers. ISSCC, pp.310 - 312, 20-24 Feb. 2011